# Image Mosaicing based on Neural Networks

Tamer A. A. Alzohairy
AssistantProfessor
Facultyofscience
Al-AZHAR University, Cairo, Egypt

Emad El-Dein H. A. Masameer
Assistant Professor
Majmaah University, Saudi Arabia
Community collage

Mahmoud S. Sayed
Demonstrator
Facultyofscience
Al-AZHAR University, Cairo, Egypt

## ABSTRACT
The main concept behind image mosaic is image registration. In image mosaicing several overlapping images are assembled in order to constitute one panoramic image. In this paper a new feature-based approach will be presented for automated image to image registration and mosaicing. The proposed method is implemented on real complex images. The proposed method is based on five main steps. First, the Harris algorithm is used to extract the feature points in the reference and sensed images. Second, feature matching is established using the Euclidean distance of the signature vectors obtained using pulse coupled neural network (PCNN). Third, transformation parameters are obtained using the least-square rule based on general affine transformation. Fourth, the image resampling and transformation are performed using bilinear interpolation to get the registered image. Finally, the mosaicing image is obtained. Experimental results show that the proposed algorithm shows excellent results when applied and tested on real complex images.

## General Terms
Image Processing, image Registration, image mosaicing and image stitching

## Keywords
Registration, Mosaicing, Reference image, Sensed image, Affine transformation, Pulse Coupled Neural Network (PCNN) and blending.

## 1. INTRODUCTION
Image registration is an inevitable problem arising in many image processing applications where it is necessary to perform aligning of two or more images of the same scene taken at different times, from different viewpoints, and/or by different sensors, into a common coordinate system thus aligning them in order to monitor subtle changes between the images. Examples of these applications include change detection using multiple images acquired at different times, fusion of image data from multiple sensor types, environmental monitoring, image mosaicing, weather forecasting, creating super-resolution images, and integrating information into Geographic Information Systems (GIS).

Image Mosaicing technology is becoming more and more popular in the fields of image processing, computer graphics, computer vision and multimedia. It is widely used in daily life by stitching pictures into panoramas or a large picture which can display the whole scenes vividly.

Nowadays almost all digital cameras come with the feature of image panorama, but still it is not giving good result and lots of improvement has to be done. So this field of image processing required lots of efforts and many new algorithms can be developed.

Automatic mosaicing of remote-sensing images is a difficult task as it must deal with the intensity changes and variation of scale, rotation and illumination of the images. Due to the diversity of images to be registered and due to various types of degradations it is impossible to design a universal method applicable to all registration tasks.

Registration techniques can be classified into two large categories: 1) Area based methods and 2) Feature based methods. In Area based methods the matching measurement is calculated by correlation equation between a template and the tested image (Peli, 1981), (Zhang, 2006); the calculation should be repeated at a variety of orientations, in order to account for possible rotational variations between the images. This method seems to be straightforward and easy to implement but, when the operation has to be repeated at each point in the second image, the amount of computer time required increases to such an extent that the method become unworkable. On the other hand, feature based techniques perform by extracting characteristic features from images and use these features to carry out the registration. The features may be highly distinctive. Points, line segments, curves are among the characteristic features generally used in image matching (Brown, 2007), (Lee, 2008), (Behrens, 2010). This paper will focus on a feature- based method to perform the Registration.

Registration based on feature method includes the following four main steps: 1) Extraction of Control Points (CPs): A set of potential CPs is selected automatically from the set of images. 2) Features CPs matching: Each feature in one image is compared with potential corresponding features in the other one. A pair of points with similar attributes is accepted as matches and they are called matching CPs. 3) Transform model estimation: Based on the set of matching CPs, the transformation model is estimated to provide the best alignment between the images. 4) Image resampling and transformation: The images are transformed based on the determined model and are resampled using an interpolation method.

In this paper, Harris detection algorithm is used to extract the corners as a CPs (Stephens, 1988). The Euclidean distance method and PCNN algorithm are used for CPs matching. The least square error is used to estimate the transformation parameters based on the matched CPs. Transformation equations are used and bilinear method is used for image resampling.

Automatic image Mosaicing or stitching is the next step after registration. In which all images are transformed according to registration parameter to a single big canvas. In this paper, to make the transition from one image to another smoother so that boundary between the two images can be removed by using image blending method.

This paper is organized as follows. Section 2 presents the proposed image Mosaicing technique. Experimental results and conclusions are given in Sections 3 and 4, respectively.

## 2. PROPOSED IMAGE MOSAICING TECHNIQUE

In this section, the proposed image mosaicing technique will be described. Figure 1 summarizes the operation of the proposed system. Five major phases are used which are: 1) feature point extraction, 2) control point correspondence, 3) transformation parameters estimation, 4) resampling and transformation, 5) image stitching and blending and 6) mosicing.

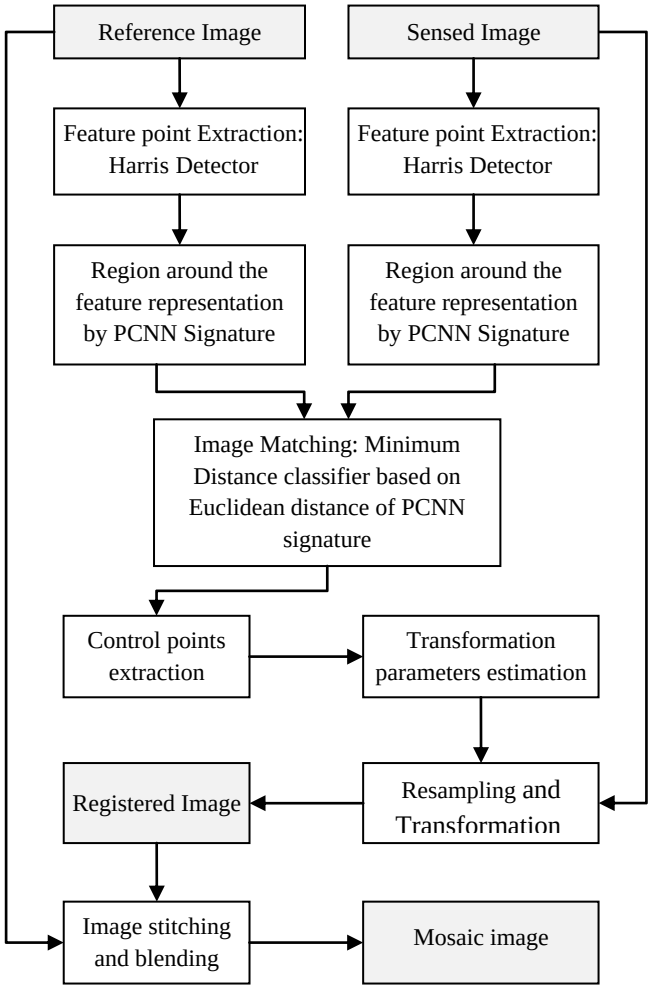


**Figure 1 Flow Chart of the proposed technique Mosaicing technique**

### 2.1 Feature point extraction using Harris corner detector

The Harris detector is a feature point extraction operator. It's one of the most widely used corner detection algorithms based on intensity, and it has a good performance on its stability and robustness (Stephens, 1988).

The Harris corner detector is based on the local autocorrelation function of a signal; where the local autocorrelation function measures the local changes of the signal with patches shifted by a small amount in different directions. The basic idea of Harris corner detector is to give a mathematical approach for determining whether a point shows significant change in all the directions by looking at intensity values within a small window and shifting the window in any direction should yield a large change in appearance.

Given a shift $[x, y]$ and a point $(u, v)$, the intensity variation $E$ can be defined as:

$$E(x,y) = \sum_{u,v} w(u,v)\,[\,I(u+x, v+y) - I(u,v)]^2 \qquad (1)$$

where $I(u,v)$ is the gray-level pixel intensity, $I(u+x, v+y)$ is the shifted pixel intensity, w specifies the image window: it is unity within a specified rectangular region, and zero elsewhere.

For small shifts, the shifted image can be approximated by a Taylor expansion

$$\boldsymbol{I(u+x, v+y) \approx I(u,v) + x\,X(u,v) + yY(u,v) + O(x^2, y^2)} \qquad (\mathbf{2})$$

where X and Y denote to the first partial derivatives in x and y, respectively. They can be approximated by

$$X = I * (-1,0,1) \;= \partial \mathrm{I}/\,\partial \mathrm{x} \qquad (3)$$

$$Y = I * (-1,0,1)^T = \partial \mathrm{I}/\,\partial \mathrm{y} \qquad (4)$$

where * is the convolution operator.

Substituting approximation Eq. (2) into Eq. (1) E can be written:

$$E(x,y) \;= \sum_{u,v} w(u,v)\,[\,xX + yY + O(x^2, y^2)]^2$$
$$= Ax^2 + 2Cxy + By^2 \qquad (5)$$

where

$$A = X^2 * w$$

$$B = Y^2 * w$$

$$C = (XY) * w$$

To achieve a more accurate estimate of the local intensity variation, a circular Gaussian window is desirable so that the Euclidean distance from the center pixel to the edge of the window is the same in all directions as given by the following formula:

$$\mathrm{w(u,v)} = \exp^{-\frac{1}{2}\frac{\mathrm{u}^2+\mathrm{v}^2}{\sigma^2}} \qquad (6)$$

Rewrite Eq. (5) in matrix form

$$E(x,y) \;\approx\; [x\ y]\, M \begin{bmatrix} x \\ y \end{bmatrix} \qquad (7)$$

Where a 2×2 matrix M is:

$$M = \begin{bmatrix} A & C \\ C & B \end{bmatrix}$$

Set $\lambda_1$ and $\lambda_2$ as the two eigenvalues of M. $\lambda_1$ and $\lambda_2$ are the rotation invariants of M and proportional to the principal curvatures of the local autocorrelation function. At this point, the flat areas, corners and edges can be judged by the value feature of $\lambda_1$ and $\lambda_2$, there are three conditions:

- If $\lambda_1 \approx 0$ and $\lambda_2 \approx 0$ then this pixel $(u, v)$ has no feature interest.
- If $\lambda_1 \approx 0$ and $\lambda_2$ has some large positive value, then an edge is detected.
- If $\lambda_1$ and $\lambda_2$ have large positive values, then corner is found.

But the eigenvalues is more expensive to compute, so Harris and Stephens (Stephens, 1988) proposed the following Corner Response measure (R) depending on matrix M according to the formula:

$$\mathrm{R} = \mathrm{Det}(M) \; - \mathrm{k} \cdot \mathrm{Tr}^2(\mathrm{M}) \qquad (8)$$

Where k is an empirical value, generally k = 0.04 ~ 0.06, $\mathrm{Det}(M)$ indicates the determinant of M, Tr(M) represents the matrix trace of M. It is attractive to use Tr(M) and $\mathrm{Det}(M)$ in the formulation, as this avoids the explicit eigenvalue decomposition of M. R is large positive for a corner region, negative with large magnitude for an edge region, small for a flat region. If R exceeds certain threshold, then taking the point as a candidate corner. The threshold must be set high enough to avoid the detection of false corners which may have a relatively large cornerness value due to noise. Finally, the corner region pixel is selected as a final corner pixel if its response is a local maximum.

## 2.2 Control Point Correspondence

After the feature points (control points) are detected from the reference and sensed images in the previous section, a correspondence mechanism between image regions around these control points must be established to match the reference and sensed images. Since the images may have translational, rotational, and scaling differences, a descriptor is needed to represent each image region in each image and this descriptor should be invariant with respect to translation, rotation, and scaling. Region similarity, for image matching, is obtained by comparing the descriptor of the region around each point in the reference and sensed images. In the following subsection the method used to find feature descriptor will be described.

### *2.2.1 The PCNN Representation of Regions*

The Pulse Coupled Neural Network (PCNN) is an artificial model developed from studies of the visual cortex of small mammals made by Eckhorn et al. (Eckhorn, 1990). This network is different from artificial neural networks in the sense that it does not require training (Haykin, 1994). The implementation of the PCNN was first carried out by Johnson (Johnson, Pulse-coupled neural nets: translation, rotation, scale, distortion, and intensity signal invariance for images, 1994).

The PCNN is a two-dimensional neural network with a single layer. Each network neuron corresponds to an input image pixel. Because of this, the structure of the PCNN comes out from the structure of input image. It's structure is shown in Fig. 2 (Wang, 2010). There are three parts that form a neuron: input part, linking part and a pulse generator. The neuron receives the input signals from feeding and linking inputs. Feeding input is the primary input from the neuron's receptive area. The neuron receptive area consists of the neighboring pixels of corresponding pixel in the input image. Linking input is the secondary input of lateral connections with neighboring neurons.

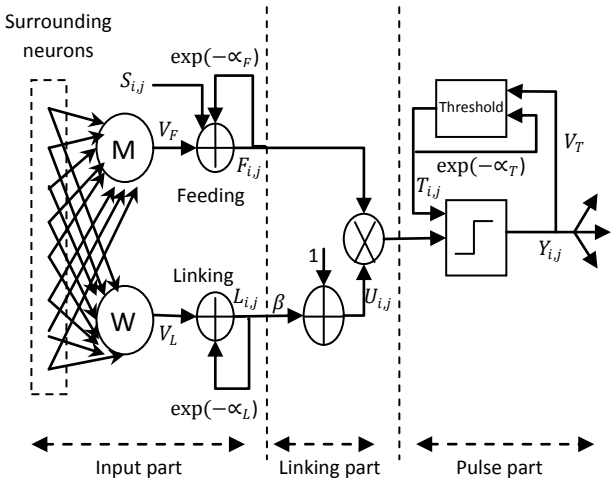


**Fig. 2 PCNN's neuron model**

The standard PCNN model is described as iteration by the following equations:

$$\mathrm{F_{ij}[n]} = \mathrm{S_{ij}} + \mathrm{F_{ij}[n-1]e^{-\alpha_f}} + \mathrm{V_f} \sum_{\mathrm{kl}} \mathrm{M_{ijkl}} * \mathrm{Y_{kl}[n-1]} \quad (9)$$

$$\mathrm{L_{ij}[n]} = \mathrm{L_{ij}[n-1]e^{-\alpha_L}} + \mathrm{V_L} \sum_{\mathrm{kl}} \mathrm{W_{ijkl}} * \mathrm{Y_{kl}[n-1]} \quad (10)$$

$$\mathrm{U_{ij}[n]} = \mathrm{F_{ij}[n](1 + \beta\, L_{ij}[n])} \quad (11)$$

$$\mathrm{T_{ij}[n]} = \mathrm{T_{ij}[n-1]e^{-\alpha_T}} + \mathrm{V_T Y_{ij}[n-1]} \quad (12)$$

$$\mathrm{Y_{ij}[n]} = \begin{cases} 1 \rightarrow \mathrm{U_{ij}[n] > T_{ij}[n]} \\ 0 \rightarrow \mathrm{Otherwise} \end{cases} \quad (13)$$

The two main components $F_{ij}$ and $L_{ij}$ are called feeding and linking in $(i, j)$ position, respectively. $U_{ij}$ is the internal activity of neuron, and $T_{ij}$ is the dynamic threshold. $Y_{ij}$ is the output of neuron. $W_{ijkl}$ and $M_{ijkl}$ are the synaptic weight coefficients, * is the convolution operator, and $S_{ij}$ is an intensity of pixel $(i, j)$ in the input matrix, usually this value is normalized. $\alpha_f$ , $\alpha_L$ and $\alpha_T$ are the decay constants of the PCNN neuron. $V_f$ , $V_L$ and $V_T$ are the magnitude scaling constants. β is the linking coefficient constant. If $U_{ij}[n] > T_{ij}[n]$, the neuron generates a pulse, called an firing time; If not, called unfiring time. After PCNN firing, the total firing number generates the output of PCNN.

The PCNN has the ability to convert a 2D image into a 1D periodic time signal which is also known as the image's signature proposed by Johnson (Johnson, Time signatures of images, 1994). In this paper, the PCNN will be used to convert image region around the control point, which is represented by two-dimensional matrix, into a sequence of temporary binary images. Each of these binary images is a matrix with the same dimension as input matrix and it is generated by group of pixels with similar intensity. The sum of all activities in specific iteration step, n, gives one value G(n) given by,

$$\mathrm{G(n)} = \sum_{\mathrm{ij}} \mathrm{Y_{ij}(n)} \quad (14)$$

which represents one feature for the classification. For N iteration steps, N features for an image region around the control point is obtained. In this paper, the obtained feature vector is used as a feature descriptor of the image region around the control point, which will be used for image matching as will be seen in next subsection 2.2.2.

Significant advantage of feature vector (generated time signal) obtained by PCNN is the invariance to rotation, scaling or translation of images (Forgáč, 1999).

### *2.2.2 PCNN signatures similarity*

After obtaining the feature descriptors (signature vectors) of the CPs, the next step is selecting the corresponding points in the reference and sensed images. Euclidean distance of the PCNN signature vectors can be used to determine the similarity between CPs in the reference and sensed images. The large value of Euclidean distance represents dissimilarity between two vectors whereas the small value gives an impression of similarity.

The Euclidean Distance (ED) between two PCNN vectors is given by:

$$ED(X,Y) = \sum_{i=1}^{N} \sqrt{(x_i - y_i)^2} \quad (15)$$

Where, $x_i$ and $y_i$ are the random variables in X and Y PCNN vectors in reference and sensed images respectively and N is the length of PCNN vector. The potential matched points are accepted by examining the following condition:

$$\frac{ED(X,Y)}{ED(X,Y')} < R_d \quad (16)$$

Where Y is a best ED match to X, $Y'$ is a $2^{nd}$ best ED match to X. A matching between points is accepted only if the ratio of nearest and next nearest feature points is less than a preset threshold $R_d$. Lower threshold, CPs matching points will be reduced, but more stable.

## 2.3 Affine transformation parameters estimation

Once the corresponding control points pairs have been found, the next essential step is to determine a spatial transformation model that maps the control points from the sensed image to the corresponding points in the reference image. The most common type of transformation models used for image registration are rigid, projective and affine. But the major issue in this step is to estimate the parameters of selected transformation model. The registration of images with rotational, translational and scaling differences can be approximated by the following general affine relationship:

$$\begin{bmatrix} x' \\ y' \\ 1 \end{bmatrix} = \begin{bmatrix} a_{11} & a_{12} & t_x \\ a_{21} & a_{22} & t_y \\ 0 & 0 & 1 \end{bmatrix} \begin{bmatrix} x \\ y \\ 1 \end{bmatrix} \quad (17)$$

Where $(x', y')$ and $(x, y)$ are two corresponding points in the reference and the sensed images, respectively. $\{a_{11}, a_{12}, a_{21}, a_{22}, t_x, t_y\}$are the transformation parameters and express scaling, rotational and translational differences between two images, these six transformation parameters are achieved by least squares method (LSM) after no less than three pairs of matching feature points which are not in the same line are determined in reference and sensed images.

Given the set of corresponding coordinates, the estimation of the affine transformation parameters is performed by using only three control point pairs having the minimum distance in the Euclidean space. These parameters are obtained by solving the following equation in a least square sense:

$$Y = Mz \quad (18)$$

where

$$Y = \begin{bmatrix} x_1' \\ y_1' \\ x_2' \\ y_2' \\ x_3' \\ y_3' \end{bmatrix} \quad M = \begin{bmatrix} x_1 & y_1 & 0 & 0 & 1 & 0 \\ 0 & 0 & x_1 & y_1 & 0 & 1 \\ x_2 & y_2 & 0 & 0 & 1 & 0 \\ 0 & 0 & x_2 & y_2 & 0 & 1 \\ x_3 & y_3 & 0 & 0 & 1 & 0 \\ 0 & 0 & x_3 & y_3 & 0 & 1 \end{bmatrix} \quad z = \begin{bmatrix} a_{11} \\ a_{12} \\ a_{21} \\ a_{22} \\ t_x \\ t_y \end{bmatrix}$$

The affine transformation parameters are found by taking the inverse of the matrix M

$$z = M^{-1}Y \quad (19)$$

Where $M^{-1}$ is the inverse of M. Based on this transformation, it is possible to map the other control points in the sensed image into the reference image.

## 2.4 Resampling and Transformation of the Sensed Image

The mapping functions constructed in subsection 2.3 are used to transform the sensed image and thus to register the images. The transformation can be realized in a forward or backward manner (Paresh M. Patel, March, 2014). Each pixel from the sensed image can be directly transformed using the estimated mapping functions. This approach, called a forward method, is complicated to implement, as it can produce holes and/or overlaps in the output image (due to the discretization and rounding). Hence, the backward approach is usually chosen. The registered image data from the sensed image are determined using the coordinates of the target pixel (the same coordinate system as of the reference image) and the inverse of the estimated mapping function. The image interpolation takes place in the sensed image on the regular grid to estimate the gray value of current position. In this way neither holes nor overlaps can occur in the output image. Common interpolation methods include: nearest neighbor interpolation, bilinear interpolation and bicubic interpolation. In the simulation experiment, given at the end of this paper, bilinear interpolation will be used.

## 2.5 Image Mosaic

Image mosaic is a process of merging two images in order to obtain a larger one. Two phases are considered in the mosaic process namely stitching of registered and reference images and image blending. Subsections (2.1) to (2.4) have shown that the images are already well registered. Using the transformation parameters obtained, the accurate position of the overlap area in both reference and registered for stitching can be determined. The problem will arise in overlapping area if the two images have different intensities. To solve this problem and improve the image mosaic quality, a fade in-out blending approach is employed (G. Lingjia, 2006). In which the overlap region pixels will add together according to the gradual change coefficient. For example, suppose two images $f_1(i,j)$ and $f_2(i,j)$, the fusion image is $f(i,j)$, can be obtained by:

$$f(i,j) = \begin{cases} f_1(x,y) & (x,y) \in f_1 \\ d_1 f_1(x,y) + d_2 f_2(x,y) & (x,y) \in (f_1 \cap f_2) \\ f_2(x,y) & (x,y) \in f_2 \end{cases} \quad (20)$$

Where $d_1$ and $d_2$ express the weight value, which are determined by overlap region width, and $d_1 + d_2 = 1$, $0 < d_1, d_2 < 1$. When $d_1$ changes slowly from 1 to 0 and $d_2$ changes slowly from 0 to 1, then the image will slowly smooth translation from $f_1(x,y)$ to $f_2(x,y)$, therefore eliminates mosaic trace (B. Triggs, 1999), (O. Pizarro, 2003), (M. Uyttendaele, 2001).

# 3. EXPERIMENTAL RESULTS AND EVALUATION

Section 3.1 demonstrates the application of the proposed method for mosaicing on two different pictures. In section 3.2 a comparison between Proposed and the Manual Registrations is presented to illustrate the effectiveness of the proposed method.

## 3.1 Data Sets and Parameters setting

In order to test the proposed image Mosaicing algorithm and demonstrate their feasibility for different type of images, results are presented in this section. Two different sets of images are presented. The first set of images is Landsat TM images from different bands acquired on (Brasilia 06-07-94) with large translation difference (Fig. 3 (a) and (b)). The second set is night view around Shizuoka-city by the PALSAR with large rotation variation (Fig. 4 (a) and (b)) which are used to show the implementation and accuracy of the proposed algorithm.

In the registration process many parameters are to be set. The success or the failure of the registration depends on these parameters. The parameters of the Harris detector were set as following: (k = 0.04, T = 10% of the maximum observed interest point strength and σ= 1) and the parameters of the PCNN were set as following: (N=30, β= 0.2, $V_L$=0.2, $V_F$=0.2, $V_\theta$=2, $\propto_F$=50, $\propto_L$=1 and $\propto_\theta$=1). During these experiments, the minimum allowed distance between two CPs is set to $d_{min} = 18$. To identify the most robust matches, the distance ratio threshold in the Euclidean space of the invariants is set to 0.5.

## 3.2 RMSE Comparison between Proposed and the Manual Registrations

Performing a registration with "success" is not sufficient to claim achieving the goal. Objective metrics must be used to evaluate the resulting mosaic. The focus is on the metric that is widely used called RMSE (Root Mean Squared Error). Assume that the transformation between the point $(x_i, y_i)$ in the sensed image and its corresponding point $(x_i', y_i')$ in the reference image is affine transformation, The RMSE at matched CPs (in pixels) between reference and registered images is defined as:

$$\text{RMSE} = \sqrt{\frac{\sum_{i=1}^{m}(\hat{x}_i - x_i')^2 + (\hat{y}_i - y_i')^2}{m}} \qquad (21)$$

Where $(x_i', y_i')$ and $(\hat{x}_i, \hat{y}_i)$ are the coordinates of the control point pairs in the reference image and the registered image (affine transformed sensed image), respectively, where $\hat{x}_i = a_{11}x_i + a_{12}y_i + t_x$ and $\hat{y}_i = a_{21}x_i + a_{22}y_i + t_y$, m is the total number of matched control points and $a_{11}$, $a_{12}$, $a_{13}$, $a_{21}$, $t_x$, $t_y$ are affine transformation parameters.

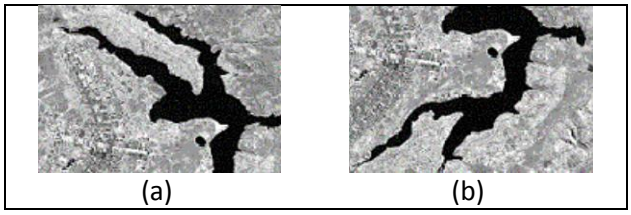


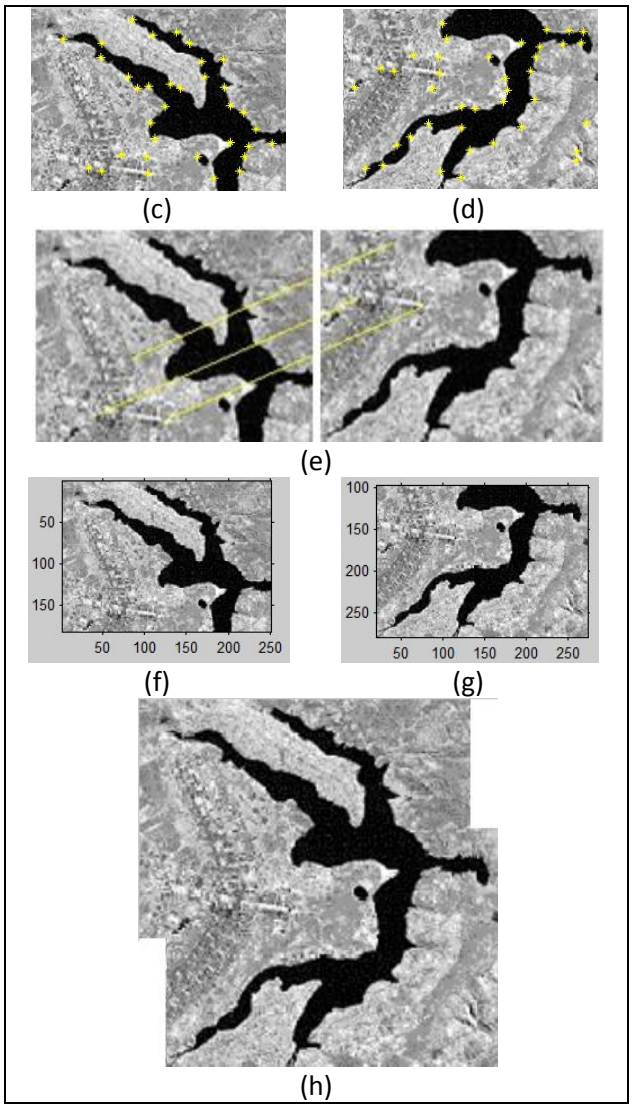


**Fig. 3 Landsat TM images from different bands acquired on (Brasilia 06-07-94) with large translation difference. (a) The reference image; (b) the sensed image; (c) the corners of (a); (d) the corners of (b); (e) the matching results of (a) and (b); (f) the reference image in a common coordinate system; (g) the registered image in a common coordinate system; (h) the mosaicing results of (a) and (b).**

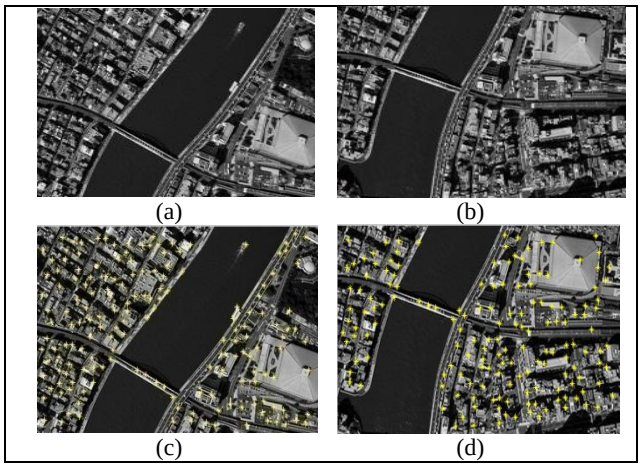

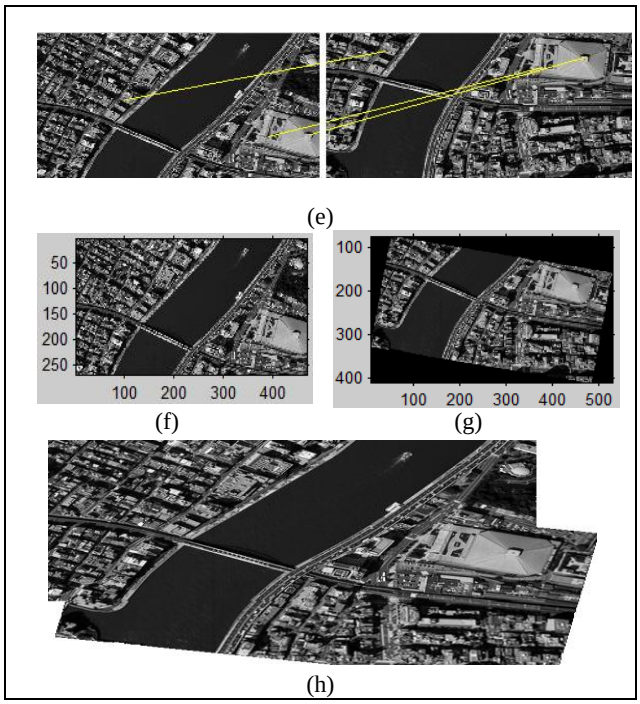


**Fig. 4 Night view around Shizuoka-city by the PALSAR with large rotation variation.(a) The reference image; (b) the sensed image; (c) the corners of (a); (d) the corners of (b); (e) the matching results of (a) and (b); (f) the reference image in a common coordinate system; (g) the registered image in a common coordinate system; (h) the mosaicing results of (a) and (b).**

The results obtained from the proposed registration method were compared with those of manual method. For a good evaluation of the performance of the proposed algorithm, distinct corner points were manually selected on the reference and sensed images given in figure 3 and that are given in figure 4. The transformation parameters and RMSEs obtained by manual registration were compared with those obtained by the proposed automatic registration method. Table I and Table II give the comparison results where the number of manually selected CPs and that generated by the proposed algorithm are kept the same in order to compare their RMSEs.

Since the determination of parameters of the general affine transformation requires no less than three control points, in this paper, three point pairs which have minimum Euclidean distance were sufficient. From Tables I and II, it is clear that the differences between the transformation parameters of the manual registration method and that of the proposed one are considerable and the transformation parameters obtained by the proposed registration approach are very close to the optimum values. Table III show the coordinates of corresponding CPs in the two pairs of images.

**Table 1Comparison Of The Proposed Automatic Registration Results With The Manual Registration Results From Figure 3**

| Method | $a_{11}$ | $a_{12}$ | $a_{21}$ | $a_{22}$ | $t_x$ | $t_y$ | RMSE |
|---|---|---|---|---|---|---|---|
| Optimal | 1.0000 | 0.0000 | 0.0000 | 1.0000 | 19.0000 | 97.0000 | 0.0000 |
| Manual | 1.0110 | -0.0027 | 0.0000 | 1.0062 | 16.8039 | 97.2030 | 0.7111 |
| Proposed Method | 1.0000 | 0.0000 | 0.0024 | 1.0000 | 19.0000 | 97.8659 | 0.1258 |

**Table 2Comparison Of The Proposed Automatic Registration Results With The Manual Registration Results From Figure 4**

| Method | $a_{11}$ | $a_{12}$ | $a_{21}$ | $a_{22}$ | $t_x$ | $t_y$ | RMSE |
|---|---|---|---|---|---|---|---|
| Optimal | 0.9848 | -0.1736 | 0.1736 | 0.9848 | 51.1056 | 73.7792 | 0.0000 |
| Manual | 0.9835 | -0.1539 | 0.1903 | 0.9161 | 50.9112 | 74.8202 | 0.5644 |
| Proposed Method | 0.9864 | -0.1737 | 0.1724 | 1.0040 | 50.9483 | 73.2880 | 0.2867 |

The coordinates of six CPs determined after application of the image matching step of the algorithm are summarized in Table III.

**Table 3Coordinates Of Corresponding Control Points In The Two Pairs Of Images**

| Control Point | Figure 3 | | Figure 4 | |
|---|---|---|---|---|
| | Reference (x,y) | Sensed (x',y') | Reference (x,y) | Sensed (x',y') |
| 1 | (115 , 161) | (96 , 64) | (146 , 123) | (102 , 32) |
| 2 | (57 , 156) | (38 , 59) | (453 , 187) | (415 , 42) |
| 3 | (87 , 108) | (68 , 11) | (381 , 192) | (345 , 59) |
| 4 | (70 , 159) | (51 , 62) | (332 , 169) | (293 , 45) |
| 5 | (89 , 143) | (70 , 46) | (451 , 244) | (423 , 98) |
| 6 | (39 , 129) | (20 , 32) | (274 , 216) | (244 ,101) |

## 4. CONCLUSION

In this paper an automatic registration technique of remote sensing images was presented. 1st Harris corner detector was used to extract the feature points. 2nd PCNN was used to deal with the large variations of scale, rotation and translation between feature points in reference and sensed images. 3rd correspondence between reference and sensed images was established. 4th affine transformation parameters were estimated by using only three pairs of CPs with minimum distance. 5th resampling and transformation of the sensed image were established. A comparison between Proposed and the Manual Registrations was presented. RMSE registration accuracy of the proposed method was 0.2867 and 0.1258 of a pixel and 0.5644 and 0.7111 for the manual method in the experiments of the two examples given in section 3.2. Clearly the image registration, using the proposed algorithm, results in a lower RMSE, and its accuracy is therefore better than that of the manual one. 6th image mosaic obtained based on the two phases namely image registration and image blending were shown in fig. 3 (h) and fig. 4 (h) which illustrate the effectiveness of the proposed method when applied on a complex images.

## 5. REFERENCES

[1] Peli, T. ( 1981). An algorithm for recognition and localization of rotated and scaled objects . Proceedings of the IEEE, 69(4), 483-485.

[2] Zhang, H., Gao, W., Chen, X., & Zhao, D. (2006). Object detection using spatial histogram features. Image and Vision Computing, 24(4), 327-341.

[3] Brown, M., & Lowe, D. G. (2007). Automatic panoramic image stitching using invariant features . International journal of computer vision, 74(1), 59-73.

[4] Lee, D. C., Kwon, O. S., Ko, K. W., Lee, H. Y., & Ha, Y. H. ( 2008, February). Image mosaicking based on feature points using color -invariant values . InComputational Imaging (p. 681414).

[5] Behrens, A., & Röllinger, H. (2010). Analysis of feature point distributions for fast image mosaicking algorithms. Acta Polytechnica, 50(4).

[6] Harris, C., & Stephens, M. (1988, August). A combined corner and edge detector . In Alvey vision conference (Vol. 15, p. 50).

[7] Eckhorn, R., Reitboeck, H. J., Arndt, M., & Dicke, P. (1990). Feature linking via synchronization among distributed assemblies : Simulations of results from cat visual cortex. Neural Computation, 2(3), 293-307.

[8] Haykin, S. ( 1994). Neural networks —a comprehensive foundationMacmillan Publishing Company . Englewood Cliffs, NJ.

[9] Johnson, J. L. (1994). Pulse-coupled neural nets : translation, rotation, scale, distortion, and intensity signal invariance for images . Applied Optics , 33(26), 6239-6253.

[10] Wang, Z., Ma, Y., Cheng, F., & Yang, L. (2010). Review of pulse-coupled neural networks. Image and Vision Computing, 28(1), 5-13.

[11] Johnson, J. L. (1994, June). Time signatures of images . In Neural Networks , 1994. IEEE World Congress on Computational Intelligence ., 1994 IEEE International Conference on (Vol. 2, pp. 1279-1284). IEEE.

[12] Forgáč, R., & Mokriš, I. (1999). Contribution to invariant image recognition using pulse -coupled neural networks . In Proc . of 5th International Conference on Soft Computing-MENDEL (Vol. 99, pp. 351-355).

[13] Patel, P. M., & Shah, V. M. (2014). Image registration techniques: a comprehensive survey. International Journal of Innovative Research and Development.

[14] Gu, L., Guo, S., Ren, R., Duan, J., Jing, W., & Zhang, S. (2006, November). A novel method of dynamic target detection. In Sixth International Symposium on Instrumentation and Control Technology : Signal Analysis, Measurement Theory , Photo-Electronic technology, and Artificial Intelligence (pp. 63570E-63570E). International Society for Optics and Photonics.

[15] Triggs, B., McLauchlan, P. F., Hartley, R. I., & Fitzgibbon, A. W. (2000). Bundle adjustment—a modern synthesis. In Vision algorithms : theory and practice (pp. 298-372). Springer Berlin Heidelberg.

[16] Pizarro, O., & Singh, H. (2003). Toward large-area mosaicing for underwater scientific applications. Oceanic Engineering, IEEE Journal of, 28(4), 651-672.

[17] Uyttendaele, M., Eden, A., & Skeliski, R. (2001). Eliminating ghosting and exposure artifacts in image mosaics. In Computer Vision and Pattern Recognition, 2001. CVPR 2001. Proceedings of the 2001 IEEE Computer Society Conference on (Vol. 2, pp. II-509). IEEE.